Received: 6 March 2021 | Revised: 23 May 2021 | Accepted: 7 June 2021

DOI: 10.1111/ejn.15352

RESEARCH REPORT

EJN European Journal of Neuroscience FENS WILEY

Decoding location-specific and location-invariant stages of numerosity processing in subitizing

Moritz F. Wurm | **Chiara F. Tagliabue** | **Veronica Mazza**

Center for Mind/Brain Sciences—CIMeC, University of Trento, Rovereto, Italy

Correspondence
Moritz F. Wurm, Center for Mind/Brain Sciences—CIMeC, University of Trento, Corso Bettini 31, 38068 Rovereto (TN), Italy.
Email: moritz.wurm@unitn.it

Funding information
Fondazione Cassa di Risparmio di Trento e Rovereto; Provincia Autonoma di Trento

Edited by: John Foxe

Abstract

Extracting the number of objects in perceived scenes is a fundamental cognitive ability. Number processing is proposed to rely on two consecutive stages: an early object location map that captures individuated objects in a location-specific way and a subsequent location-invariant representation that captures numerosity at an abstract level. However, it is unclear whether this framework applies to small numerosities that can be individuated at once ("subitized"). Here, we reanalyzed data from two electroencephalography (EEG) experiments using multivariate pattern decoding to identify location-specific and location-invariant stages of numerosity processing in the subitizing range. In these experiments, one to three targets were presented in the left or right hemifield, which allowed for decoding target numerosity within each hemifield separately (location specific) or across hemifields (location invariant). Experiment 1 indicated the presence of a location-specific stage (180–200 ms after stimulus), followed by a location-invariant stage (300 ms after stimulus). A time-by-channel searchlight analysis revealed that the early location-specific stage is most evident at occipital channels, whereas the late location-invariant stage is most evident at parietal channels. Experiment 2 showed that both location-specific and location-invariant components are engaged only during tasks that explicitly require numerosity processing, ruling out automatic, and passive recording of numerosity. These results suggest that numerosity coding in subitizing is strongly grounded on an attention-based, location-specific stage. This stage overlaps with the subsequent activation of a location-invariant stage, where a full representation of numerosity is finalized. Taken together, our findings provide clear evidence for a temporal and spatial segregation of location-specific and location-invariant numerosity coding of small object numerosities.

KEYWORDS
EEG, enumeration, MVPA, numerosity, subitizing

Abbreviations: ANOVA, analysis of variance; EEG, electroencephalography; ERP, event-related potential; LDA, linear discriminant analysis; MVPA, multivariate pattern analysis.

1 | INTRODUCTION

How the brain processes numerosity, for instance, during object enumeration, has interested cognitive neuroscientists for decades. According to traditional models (Dehaene & Changeux, 1993; Meck & Church, 1983; Verguts & Fias, 2004; Zorzi et al., 2005), numerosity coding is the result of a multistage process that transforms the initial nonsymbolic sensory input into an abstract representation of the number of an object set (but see Dakin et al., 2011). These models rely on a core assumption about a (broad) distinction between location-specific and location-invariant stages of numerosity processing.

The location-specific stage ("object location map") represents the position of the relevant items in a "normalized" fashion (i.e., irrespective of other physical factors, such as size), so that their numerosity is reflected in the number of spatially distinct positions occupied by the elements. Psychophysical (Burr & Ross, 2008) and computational (Stoianov & Zorzi, 2012) studies have further supported the plausibility of a spatially selective processing stage of numerosity coding. This stage is not specifically tuned to numerosity but provides a representation that is shared by many visuospatial functions, including numerosity coding (Dehaene et al., 2003). In (a) subsequent location-invariant stage(s) of numerosity processing, the numerosity of the set of objects is represented in an abstract way, independently of the location in the visual field. The final output is a representation of the specific numerical value of the object set (Verguts & Fias, 2004).

Neuroimaging findings (Eger et al., 2009, 2015; Roggeman et al., 2011) have lent initial support to this distinction, in particular for the existence of location-invariant numerosity representations in parietal areas (Eger et al., 2015; Harvey & Dumoulin, 2017; Harvey et al., 2015; Viswanathan & Nieder, 2020). However, studies that aimed at providing evidence for a two-stage model by isolating and segregating both location-specific and location-invariant stages are scant. Additionally, anatomical segregation alone could prove difficult to reach a firm conclusion about the existence of two independent stages of numerosity coding. For instance, whether the stages operate simultaneously or sequentially cannot be easily addressed on the basis of anatomical segregation. Thus, to demonstrate the existence of a sequential two-stage processing mode of numerosity, the higher time resolution provided by electroencephalography (EEG) may offer more stringent evidence for a temporal dissociation between location-specific and location-invariant stages of numerosity processing.

Some previous EEG findings could be compatible with the existence of either an object location map in early stages of processing (although with disagreement on the exact time window, i.e., from about 75 to 150 ms after stimulus; see Hyde & Spelke, 2009; Park et al., 2016, respectively) or a more abstract representation of numerosities (occurring at approximately 250–300 ms; see Libertus et al., 2007). However, there has been no systematic attempt to directly test in a single study the time course of location-specific versus location-invariant components of numerosity coding. The only recent exception in this direction (Fornaciai et al., 2017) found an inversion of the early EEG responses in posterior areas (100 ms after display onset) for the numerosities in the approximate number system range (i.e., 8–32) for upper versus lower stimulus presentations, pointing towards location-specific numerosity coding. This effect was followed by a second response occurring at later time (200 ms after stimulus onset), which was sensitive to the numerosities in a location-invariant fashion. However, this is so far the only electrophysiological support to the existence of a dual-mode coding of numerosity, which may become problematic for the credibility of models of numerosity coding. Moreover, the study focused on a specific numerosity range, the typical one used in estimation tasks. Therefore, whether the dual-mode coding of numerosity applies to all numerosities, and to small object sets in particular, has remained elusive.

Small object sets have a special status in enumeration tasks, leading to the so-called subitizing effect (Kaufman et al., 1949; Mandler & Shebo, 1982). Subitizing is the effortless processing of a small set of items (up to three to four elements), and it seems to be a universal trait of humans (including infants) and several animal species (for a review, see Feigenson et al., 2004). According to some influential models (e.g., Feigenson et al., 2004; Piazza, 2010; Trick & Pylyshyn, 1994), the effect is considered a main feature of exact enumeration (as opposed to approximate enumeration that applies to larger numerosities), wherein the visual system is capable of individuating each element of the relevant set to ensure that it is enumerated once and only once (Pylyshyn, 2001). Moreover, previous studies (Ansari et al., 2007; Cavanagh & Alvarez, 2005; Vetter et al., 2011; Xu & Chun, 2009) have highlighted a strong link between object individuation and attention, thus characterizing subitizing as an attention-based effect. For all these reasons, subitizing seems to rely on a different mechanism with respect to enumeration or estimation of larger quantities or to implicit (passive) numerosity coding. Does subitizing still reflect the outcome of a dual-mode coding of numerosity? In other words, is there a two-stage process in subitizing, as predicted by models of numerosity perception?

Two studies provided an electrophysiological distinction between subitizing and the processing of larger numerosities (Fornaciai & Park, 2017; Hyde & Spelke, 2009), with small numerosities activating stages in the mid-latency range (i.e., around 150–180 ms after stimulus onset). The distinction was taken as further support to the suggestion that the neural circuitry dedicated to small numerosity coding is different from the mechanism for estimating larger numerical quantities. However, this distinction was not directly grounded on the test for a location-specific versus location-invariant component. Therefore, whether the activation of the mid-latency stages (i.e., approximately 180 ms after stimulus onset) found in these previous studies for subitizing still rely on a location map has remained elusive.

Overall, because no direct test for temporal segregation of a location-specific versus location-invariant component in subitizing has been conducted so far, it has remained unclear the extent to which the dual-mode coding of numerosity applies to subitizing. Here, we provide direct evidence for a temporal (and spatial) segregation of the stages involved in subitizing. To this aim, we exploited data from an EEG study on individuation of small numerosities (Mazza & Caramazza, 2011). This study focused on the N2pc (Eimer, 1996) as an electrophysiological marker of target individuation and their variation in numerosity. The (traditional) approach for the event-related potential (ERP) analysis of lateralized responses used in that study could not be applied to segregate location-specific versus location-invariant stages. However, as we elaborate below, the experimental design is optimally suited for using multivariate pattern analysis (MVPA) to test for a dissociation between location-specific and location-invariant neural numerosity representations in terms of time course and temporal order. Crucially, the objects to be enumerated were presented in either the left or right hemifield. By decoding target numerosity within each hemifield separately (location specific) or across hemifields (location invariant), we were able to disentangle the time courses of location-specific versus location-invariant stages: to isolate the location-specific stage, we trained a classifier to discriminate targets appearing in the left hemifield and tested the classifier using targets appearing in the same hemifield. The same was done for targets appearing in the right hemifield. Importantly, the location-specific stage is expected to be processed mainly contralaterally to the hemifield. We therefore tested for the lateralization of location-specific numerosity decoding effects, which served as the critical criterion for the location-specific stage: an interaction of decoding of left versus right target numerosities in the right versus left hemisphere can only be explained by location-specific numerosity representations. Testing for this interaction is crucial because within-hemisphere decoding can also be driven by location-invariant numerosity representations. This approach thereby provides a highly selective test that goes beyond previous attempts to isolate location-specific numerosity representations. To isolate the location-invariant stage, we trained a classifier to discriminate targets appearing in the left hemifield and tested the classifier using targets appearing in the right hemifield (and vice versa). Thus, numerosity decoding across hemifields can only be explained by location-invariant numerosity representations. Taken together, this decoding approach provides the critical selectivity for segregating location-specific and location-invariant stages. Finally, we performed a time-by-channel searchlight analysis for location-specific and location-invariant numerosity decoding to thereby test for the spatial segregation of the dual-mode coding of numerosity.

Following the literature on the subitizing effect in human adults, where the relevant items have to be enumerated (e.g., Mandler & Shebo, 1982; Trick & Pylyshyn, 1993), Experiment 1 used an explicit enumeration task requiring to report the number (or to detect a specific numerosity) of targets presented among distracters. The use of distracting objects is not a specific requirement for the occurrence of subitizing. In fact, in the original study (Mazza & Caramazza, 2011), the presence of distractors was mainly motivated by the need to have a context similar to most of the EEG studies on attentive individuation. However, it is noteworthy that the inclusion of distracting objects should not modify the nature of the subitizing effect, as shown by previous research (Mazza et al., 2013; Trick & Pylyshyn, 1993). In addition, the use of distracter elements ensures that the overall area occupied by the items remains constant despite the variation in target numerosity. This allowed us to (at least partially) exclude an explanation of the effects in terms of sensory-based coding, namely, that any distinction across numerosities could be exclusively related to a passive encoding of the variation in continuous magnitudes, such as overall area (namely, the area occupied by all the objects), that typically covary with variation in numerosity.

Experiment 2 was conducted to test the extent to which the effects found in Experiment 1 were ascribed to "explicit" enumeration (the typical task used to study subitizing in human adults, e.g., Trick & Pylyshyn, 1994), or to an automatic, passive encoding of target numerosities and their variation, as typically seen in studies with larger object sets (e.g., Piazza et al., 2004).

2 | METHODS

Data were taken from Mazza and Caramazza (2011) and analyzed here with a multivariate decoding approach to characterize the generalization profiles of numerosity representations at different time points. Thus, the research question and the results obtained by the analyses used in the present study are fully independent from Mazza and Caramazza (2011). Data of Experiment 1 were originally collected in two separate experiments (Experiments 1 and 3, see Mazza & Caramazza, 2011, hereafter Experiments 1a and 1b). Because both experiments rely on similar enumeration processes, as also indicated by both behavioral and EEG results (Mazza & Caramazza, 2011), they were collapsed to increase power for the EEG decoding procedure. In addition, it was verified that there were no significant differences in decoding accuracies between the two experiments (see Section 2.4 for details).

2.1 | Participants

Twenty-four right-handed volunteers, with normal or corrected-to-normal vision and no color blindness, recruited among students of the University of Trento, participated in Experiment 1 (collapsed Experiments 1a and 1b: 20 females; mean age 20.8 years) and 12 in Experiment 2 (all right-handed, eight females; mean age 22 years). They all provided their written informed consent. The experimental procedures were conducted in accordance with the declaration of Helsinki guidelines and approved by the Ethics Committee for research involving human participants at the University of Trento, Italy.

2.2 | Stimuli and procedure

In both Experiments 1 (Experiments 1a and 1b) and 2, on each trial, red and green diamond shapes were presented. The display contained 16 diamonds, eight in each hemifield, and appeared for 150 ms. Participants had up to 1500 ms to respond, and the intertrial interval lasted 1500 ms (Figure 1a). In each trial, in one hemifield, one, two, or three diamonds had a unique color (either red or green), serving as targets. Experiments 1a and 2 included also zero-target trials, which were removed for all analyses, except for a control analysis for Experiment 2. In Experiments 1a and 2, there were 300 and 200 trials for each numerosity from 1 to 3 and 300 and 600 trials for zero-target condition, respectively. In Experiment 1b, there were 416 trials per numerosity (from 1 to 3). In Experiment 1a, participants had to report the exact number (0/1/2/3) of targets presented. In Experiment 1b, in each block, participants decided (Yes/No) whether a specific target numerosity (designated at the beginning of each block) was presented. In Experiment 2, the task was to decide (Yes/No) whether at least one target was shown on display. For further specific details, see Mazza and Caramazza (2011).

2.3 | EEG recording and data preprocessing

The EEG signal was recorded with BrainAmp system (Brain Products GmbH, Munich, Germany—BrainVision Recorder) from 25 electrodes (including PO7 and PO8) with a 1000-Hz sampling rate (bandpass filter: 0.01–200 Hz). A right earlobe channel was used as online reference, and horizontal eye movements were recorded through two channels positioned on the outer canthi of both eyes. The continuous EEG signal was off-line processed using EEGLAB (Delorme & Makeig, 2004) and ERPLab (Lopez-Calderon & Luck, 2014). The signal was down-sampled to 250 Hz, low-pass filtered (40 Hz), and then re-referenced to the average of both earlobe channels. Trials yielding correct responses were segmented from −100 to 600 ms with respect to stimulus onset and baseline corrected over the 100 ms preceding the stimulus. Finally, those trials containing artifacts were removed (when HEOG exceeded ±30 μV and/or any other channel exceeded ±80 μV; on average, 8.8% of trials were excluded). After preprocessing, in Experiment 1a, for each numerosity, the following average number of trials was used for the analysis: 278.75 (one target), 269.25 (two targets), and 288.25 (three targets); in Experiment 1b: 400 (one target), 392.44 (two targets), and 405.81 (three targets); and finally, in Experiment 2: 191.83 (one target), 193.67 (two targets), 190.17 (three targets), and 578.5 (zero target).

2.4 | Multivariate pattern classification

To decode numerosity from EEG signals, the CoSMoMVPA Toolbox (Oosterhof et al., 2016) was used. The procedure for Experiments 1 and 2 was identical: for each participant, channel, and condition, we generated pseudotrials that were used for training and testing a linear discriminant analysis (LDA) classifier: first, we randomly divided the data into eight chunks. For each chunk, we then generated an equal number of pseudotrials consisting of the average of two trials each.

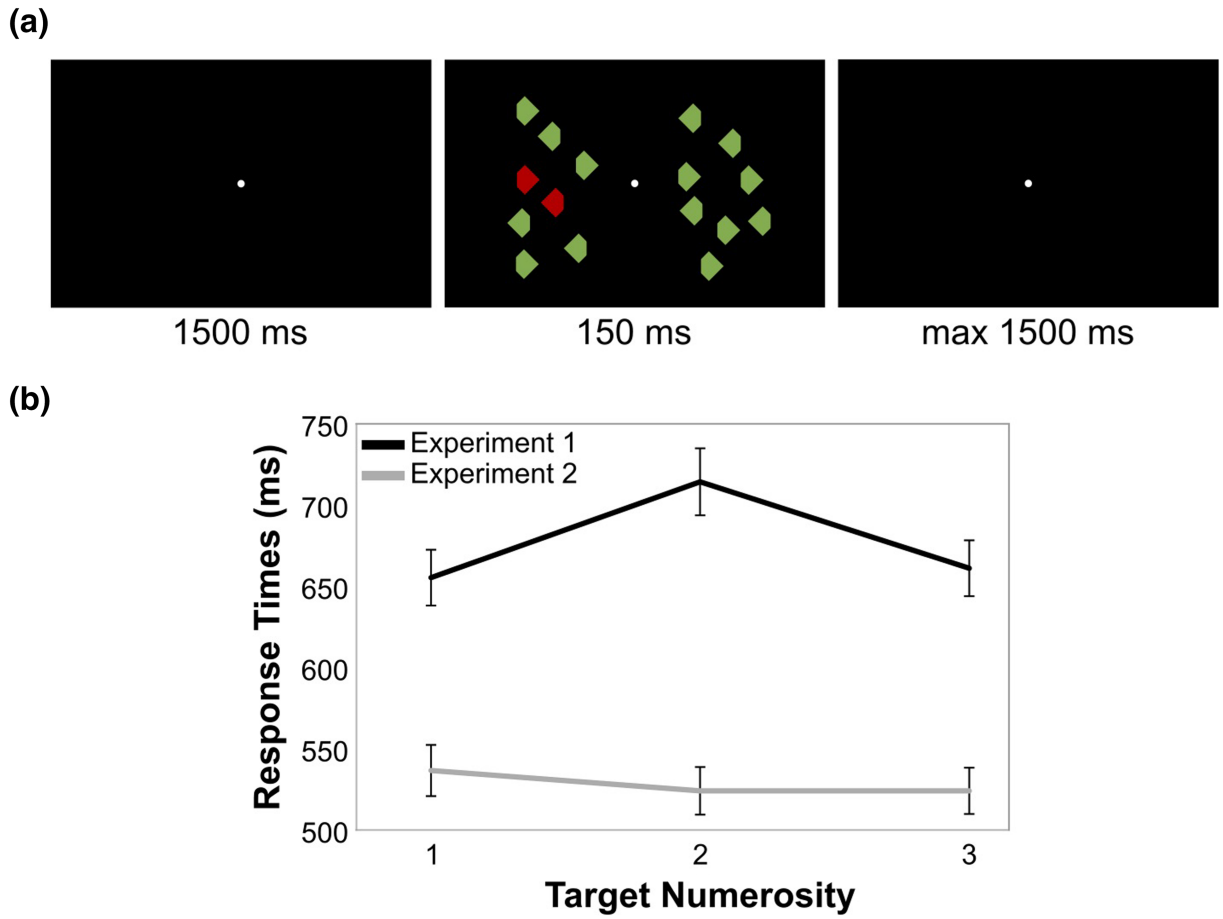

FIGURE 1 Stimuli and behavioral results. (a) Temporal sequence of a trial. (b) Mean response times of Experiments 1 and 2. Vertical bars represent standard error of the mean

We resampled each trial with a maximum number of three times, that is, each trial was averaged with another, randomly selected trial maximally three times. Moreover, the partitions for classification training and testing were balanced in terms of trial number within each participant (using the Matlab function cosmo_balance_partitions of the CoSMoMVPA Toolbox) to ensure that for each condition, the same number of pseudotrials was entered into classification. As a result, the number of trials for each chunk and numerosity was identical. Each chunk contained on average 674 pseudotrials (225 per condition; range 184–248) for Experiment 1 and 712 pseudotrials (237 per condition; range 112–288; ranges reflect the variance between participants) for Experiment 2. Because resampling was done for each chunk separately, data for training and testing classification were guaranteed to be independent.

A temporal searchlight MVPA was performed using a temporal radius of two time bins (one bin = 4 ms), that is, for each time point, EEG data from 2 preceding to 2 following time points was used for classification (covering a range of 20 ms).

Location-specific numerosity representations should be lateralized to the contralateral hemisphere, that is, numerosity of left targets should be represented in the right hemisphere (and thus be decoded better from right electrodes) and vice versa for right targets. Because within-hemifield decoding could in principle be driven by both location-specific and location-invariant numerosity representations, the interaction of hemifield- and hemisphere-specific decoding thus provides a compelling proxy for location-specific coding of numerosity.

Numerosity decoding was performed using either all EEG channels or for left and right EEG channels separately (excluding channels along the midline), using the following multiclass decoding schemes: (1) for the *location-specific decoding*, we used all channels to decode targets for each hemifield separately, that is, we trained and tested the classifier on targets appearing on the left side only, and in a separate classification, we did the same for targets appearing on the right side. Classification performance was assessed using leave-one-chunk-out cross validation: the classifier was trained to decode numerosity using data of seven out of the eight

chunks and tested on its ability to decode numerosity using data of the held-out chunk. This was iterated eight times, leaving out each chunk once. Resulting decoding accuracies were then averaged across the iterations and across hemifield. (2) For the *location-invariant decoding*, we trained the classifier, using all channels, to discriminate the numerosity of left targets and tested the classifier on its ability to decode numerosity of right targets. The same was done vice versa, and resulting decoding accuracies were averaged. (3) For the *location-specific/hemisphere-specific decoding*, we repeated the location-specific decoding for left and right channels separately, that is, for targets appearing on the left side, we used either right (contralateral) or left (ipsilateral) channels and vice versa for targets appearing on the right side. Resulting decoding accuracies were averaged only across the iterations but not across hemifield or hemisphere.

For each decoding scheme, resulting accuracy time courses were entered into one-tailed one-sample *t* tests across participants against chance (=33.3%). For the *location-specific/hemisphere-specific decoding*, we also performed repeated-measures ANOVA with the factors HEMIFIELD and HEMISPHERE. To correct for multiple comparisons, we used a cluster-based Monte Carlo simulation algorithm as implemented in the CoSMoMVPA Toolbox (Oosterhof et al., 2016). We used a threshold of $p = 0.05$ (one-tailed) at the cluster level, an initial threshold of $p = 0.001$ per time bin, and 10,000 iterations of Monte Carlo simulations. Based on the initial *p* threshold, it is estimated how many time bins would be expected to pass this threshold by chance (i.e., are false positives). Monte Carlo simulations are used to estimate cluster sizes of temporally adjacent false positives. This is done by randomly flipping the sign of decoding accuracies (over all time points, which preserves the temporal smoothness in individual subjects) after subtracting decoding at chance (i.e., 1/3 for numerosity decoding). The resulting null distribution of cluster sizes is then compared with the actually observed cluster size (at the initial *p* threshold) to compute the likelihood that an observed cluster occurs by chance (i.e., the cluster threshold).

To test whether there were any significant differences between Experiments 1a and 1b, we performed independent *t* tests between decoding accuracy time courses from Experiments 1a and 1b for each decoding scheme (*location-specific decoding* and *location-specific/hemisphere-specific decoding*). Resulting *t* time courses were corrected for multiple comparisons as described above. For all of the decoding schemes, there were no significant differences between Experiments 1a and 1b.

Finally, we computed Bayes factors (BFs) for Experiment 2 to estimate the likelihood for the presence versus absence of decoding accuracies different from chance. Bayesian statistical analyses were computed using the bayesFactor toolbox for Matlab (https://github.com/klabhub/bayesFactor), with a default Cauchy prior width of $r = 0.707$ for effect size.

2.5 | Time-by-channel searchlight MVPA

To provide further evidence for a segregation between the location-specific and location-invariant stages and to investigate the topographical distribution of these stages on the scalp, we performed a searchlight analysis across time and EEG channels. This was realized by crossing the feature neighborhoods of the temporal dimension (radius = two time bins around each center time bin) and the spatial dimension (radius = two EEG channels around each center channel), resulting in time-by-channel neighborhoods (Oosterhof et al., 2016). For each time-by-channel neighborhood, we performed the location-specific and location-invariant numerosity decoding using the same parameters and procedures as described above, except that for the location-specific decoding, resulting accuracy maps were not averaged across hemifields. Resulting time-by-channel maps were corrected for multiple comparisons using cluster-based Monte Carlo simulations as described above, with the specification that clusters do not have to be connected by neighboring time points, which increases the threshold to reach significance but allows more accurate inferences about time points of significant effects (Oosterhof et al., 2016). The time-by-channel accuracy maps were converted into FieldTrip structures to generate topographical plots (Oostenveld et al., 2011) for visualization.

3 | RESULTS

3.1 | Behavioral results

The main findings from the behavioral analyses are summarized below and shown in Figure 1b. For detailed descriptions, see Mazza and Caramazza (2011). For Experiments 1 (a and b) and 2, proportion of correct responses and reaction times (RTs, calculated for correct responses between 200 and 1500 ms) were measured. As Experiments 1a and 1b yielded comparable results, the data were collapsed. All values were submitted to repeated-measures ANOVAs with numerosity (three levels) as within-subjects factor.

In Experiment 1, the ANOVA on RTs revealed a significant effect of Target numerosity ($F(2, 46) = 40.002$,

$p < 0.001$, $\eta_p^2 = 0.635$). RTs were slower for two than one and three targets ($ps < 0.001$). Also for accuracy, target numerosity was significant ($F(2, 46) = 21.020$, $p < 0.001$, $\eta_p^2 = 0.478$). In line with RTs, the proportion of correct responses was lower for two than one and three targets ($ps < 0.001$). In Experiment 2, the ANOVA on RTs only showed a trend towards significance for target numerosity ($F(3, 33) = 3.259$, $p = 0.053$, $\eta_p^2 = 0.229$). RTs were faster when two and three targets were presented compared with one-target condition ($ps < 0.039$). No effect was significant with accuracy data ($p = 0.095$).

3.2 | EEG results

3.2.1 | Experiment 1

To investigate the time course of location-specific and location-invariant numerosity representations, we first performed multivariate pattern decoding on target numerosity (1, 2, and 3) for each hemifield separately (within-hemifield decoding) and across hemifields, respectively. For the location-specific decoding, we trained and tested the classifier on targets from the same hemifield. For the location-invariant decoding, we trained the classifier on left targets and tested it on right targets and vice versa. All channels were used in this analysis. For each time point and decoding test, one-tailed one-sample t tests were performed. Location-specific and location-invariant decoding accuracies were compared using paired samples t tests. We found that location-specific numerosity representations were reliably present from 180 ms after stimulus (peaking around 270–320 ms after stimulus onset). Location-invariant representations started at approximately 300 ms, peaking much later (around 550 ms after stimulus onset). Significant differences between location-specific and location-invariant decoding started at 184 ms after stimulus onset (Figure 2a and Table 1).

Whereas the location-invariant decoding provides unambiguous evidence about location-invariant numerosity representations, the location-specific decoding could theoretically also be driven by ipsilateral (and thus location invariant) numerosity representations. To provide additional, compelling evidence for the location-specific decoding, we tested whether the location-specific decoding is stronger for contralateral as compared with ipsilateral channels with regard to the hemifield in which the targets appeared. We therefore repeated the location-specific numerosity decoding for left and right channels separately. As predicted, we found stronger decoding in contralateral versus ipsilateral channels (Figure 2b and Table 1). A repeated-measures ANOVA with the factors HEMIFIELD (left and right targets) and HEMISPHERE (left and right channels) revealed a significant interaction between HEMIFIELD and HEMISPHERE after 224 ms, with a second peak at 508 ms after stimulus onset (significant interaction effect ranges [min–max]: $F(1, 23) = 7.9–44.4$, $p = 9.7e\text{-}03–8.4e\text{-}07$, $\eta_p^2 = 0.26 – 0.66$).

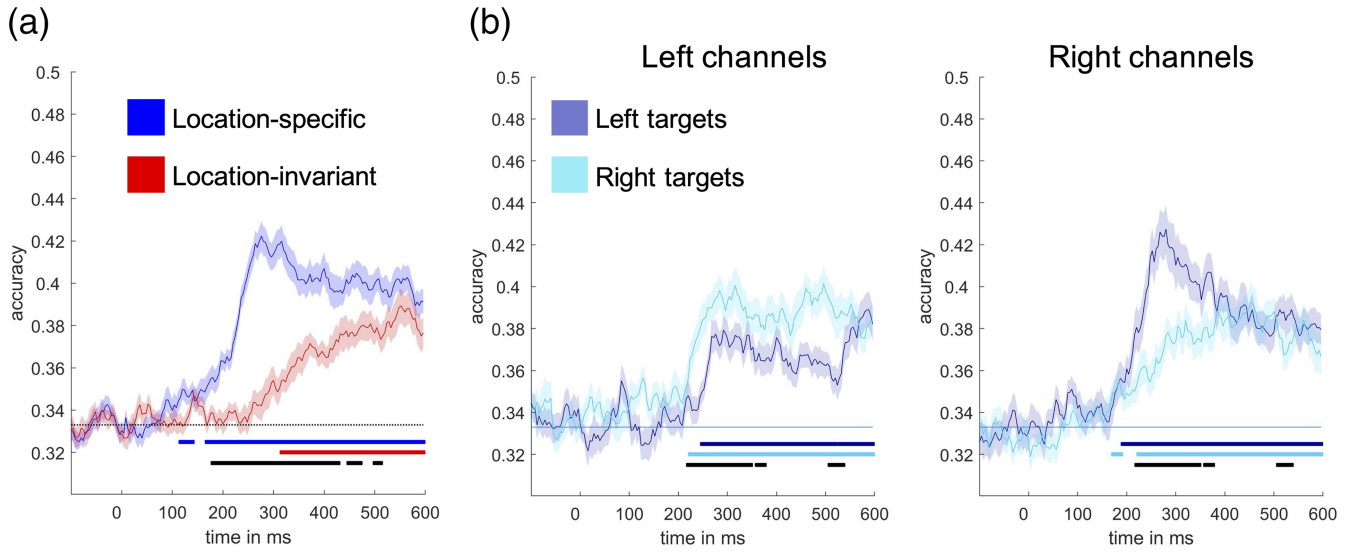

FIGURE 2 Numerosity decoding in Experiment 1. (a) Location-specific and location-invariant decoding using all channels. The black horizontal line indicates significant differences between location-specific and location-invariant decoding. (b) Location-specific decoding for left and right channels separately. Black horizontal lines indicate a significant interaction between HEMIFIELD and HEMISPHERE. In both (a) and (b), colored horizontal lines indicate significant decoding accuracies above chance. All significance tests are corrected for multiple comparisons

TABLE 1 Statistical information about decoding onsets, peaks, and significant time windows for the different numerosity decoding analyses in Experiment 1

			Location specific/hemisphere specific			
	Location specific	**Location invariant**	**Left hemisphere/ left hemifield**	**Left hemisphere/ right hemifield**	**Right hemisphere/ left hemifield**	**Right hemisphere/ right hemifield**
Decoding onset (s)	0.116	0.316	0.248	0.224	0.192	0.172
Onset accuracy ± SEM	0.35 ± 0.0045	0.35 ± 0.0056	0.35 ± 0.0052	0.35 ± 0.0078	0.35 ± 0.0073	0.35 ± 0.0057
Peak decoding (s)	0.276	0.552	0.588	0.496	0.28	0.452
Peak accuracy ± SEM	0.42 ± 0.0071	0.39 ± 0.0081	0.39 ± 0.0086	0.40 ± 0.0085	0.43 ± 0.0116	0.39 ± 0.0086
Max–min $t(23)$	2.8–14.1	3.4–8.2	3.1–7.2	4.5–8.7	1.4–9.6	2.9–9.1
Min–max p	4.9e-03–3.9e-13	1.1e-03–1.3e-08	2.3e-03–1.2e-07	8.8e-05–4.6e-09	9.1e-02–8.9e-10	4.5e-03–2.1e-09

Abbreviation: SEM = standard error of mean.

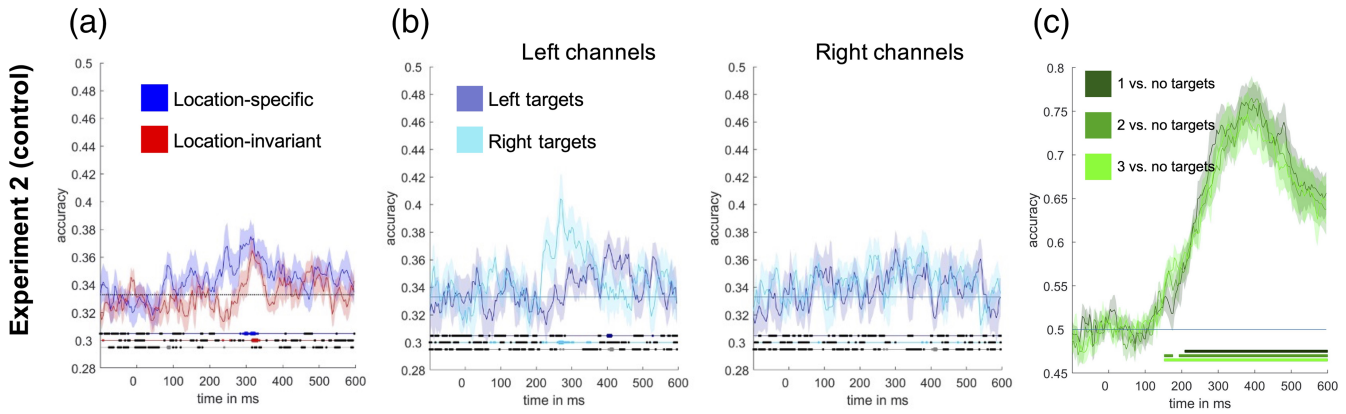

FIGURE 3 Numerosity decoding in Experiment 2 (control experiment). (a) Location-specific and location-invariant decoding using all channels. (b) Location-specific decoding for left and right channels separately. In both (a) and (b), no significant decoding accuracies above chance or interactions were observed. To highlight trends for the presence or absence of numerosity decoding, Bayes factors (BFs) are plotted as red/blue/gray lines (evidence for H1, BFs > 3; thick lines BFs > 10; gray lines indicate differences between location-specific and location-invariant decoding) or black lines (evidence for H0; BFs < 0.3). (c) Decoding of each target numerosity versus zero-target trials (task-relevant dimension). Colored horizontal lines indicate significant decoding accuracies above chance. All significance tests are corrected for multiple comparisons

3.2.2 | Experiment 2

Experiment 2 was identical to Experiment 1 except that participants just had to indicate the presence or absence of targets irrespective of their numerosity. For all numerosity decoding tests, no significant effects were observed, and apart from trends for location-specific and location-invariant decoding around 300 ms, decoding accuracies fluctuated around chance (Figure 3a,b).

3.2.3 | Control analyses

Because the sample size was lower in Experiment 2 ($N = 12$) than in Experiment 1 ($N = 24$), we also tested for the possibility that Experiment 2 did not have enough power to detect location-specific and location-invariant numerosity representations. We used three control analyses: first, we computed Bayesian comparisons to test the strength of evidence for H1 and H0. This revealed trends for location-specific and location-invariant numerosity decoding around 300 ms and for location-specific/hemisphere-specific decoding (right targets) around 280–300 ms after stimulus onset (BFs > 10). Importantly, the decoding profiles did not correspond with the decoding profiles of Experiment 1. Moreover, several time windows that overlapped with the location-specific and location-invariant stages found in Experiment 1 showed stronger evidence for H0 (BFs < 0.3), which argues against the possibility that

Experiment 2 targeted similar location-specific and location-invariant stages, and that they were not detected because of weaker effects due to lower power. Second, to test whether the EEG data in Experiment 2 is generally sufficiently powerful for successful decoding, we tested whether targets (1, 2, and 3) could be discriminated from zero-target trials. Because this comparison targeted task-relevant information, we would expect that each of the numerosities can be successfully discriminated from zero-target trials. This was the case for each numerosity. Notably, each numerosity could be decoded equally well from zero-target trials, further indicating that the three numerosities were not processed differently (Figure 3c). Third, to test whether 12 participants are generally sufficient to demonstrate significant effects for location-specific and location-invariant numerosity decoding, we used a bootstrapping approach, in which we randomly selected 12 participants of Experiment 1 and repeated the statistical analysis. In each of 1000 iterations, we replicated the significant decoding of location-specific and location-invariant numerosity representations (for further information on this analysis, see supporting information and https://osf.io/kb23q/). Taken together, these results suggest that the numerosity representations decoded in Experiment 1 were not due to a passive processing of object numerosity but depended on the explicit requirement to enumerate the relevant objects.

3.2.4 | Time-by-channel searchlight MVPA

To corroborate the identified segregation between the location-specific and location-invariant stages and to provide a coarse idea about the location of these stages in channel space, we performed a time-by-channel searchlight analysis. The resulting topographical maps for the location-specific numerosity decoding in Experiment 1 revealed classification accuracies above chance that peaked around posterior channels of the contralateral hemisphere from around 200 to 300 ms (Figure 4, top and middle rows). Later decoding was more widespread and less lateralized, peaking around central channels. The location-invariant decoding started later (250 ms), with bilateral peaks around more anterior parietal channels (sparing the most posterior channels that revealed the strongest effects in the location-specific decoding; Figure 4, bottom row), suggesting not only a temporal but also a spatial segregation of the two stages. Experiment 2 revealed no significant effects of location-specific and location-invariant decoding.

4 | DISCUSSION

The human brain is endowed with the ability to efficiently enumerate up to three to four objects, a phenomenon known as subitizing effect (Kaufman et al., 1949). Despite being a pervasive phenomenon, some aspects of subitizing have remained unclear. By means of EEG decoding, the present study addressed whether a crucial aspect of the neural architecture of numerosity representation, namely, the presence of a dual-stage numerosity mode, also applies to the special case of subitizing. Specifically, decoding numerosity within each hemifield separately and testing for significantly stronger contralateral versus ipsilateral numerosity discrimination allowed

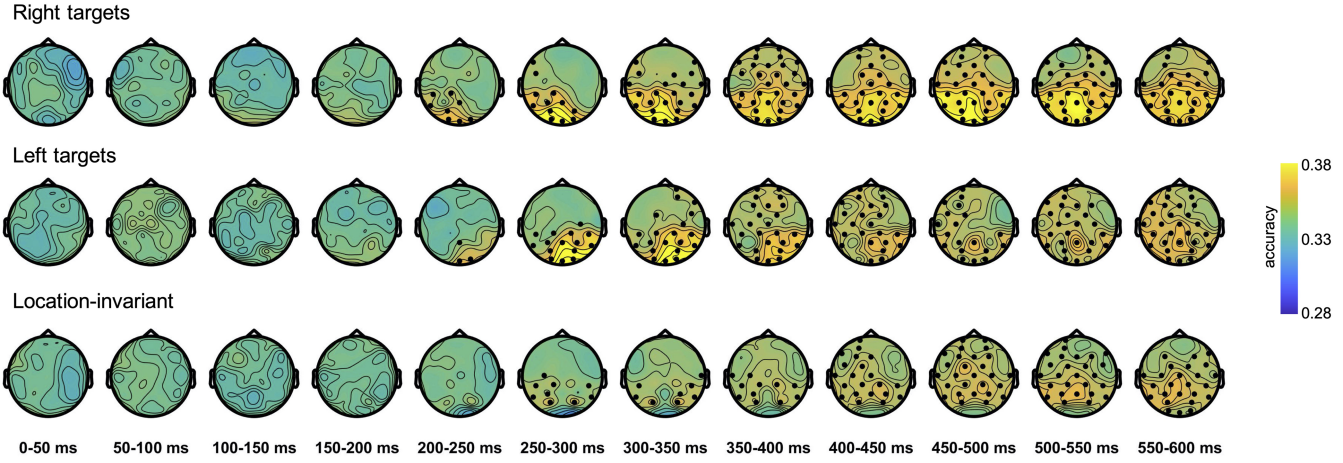

FIGURE 4 Searchlight multivariate pattern analysis (MVPA) for location-specific and location-invariant numerosity representations in Experiment 1. For visualization purposes, time-by-channel searchlight maps were averaged across time every 50 ms. Black dots indicate center electroencephalography (EEG) channels that revealed significant numerosity decoding accuracies above chance (corrected for multiple comparisons) in at least one time point (i.e., 4 ms) within each 50-ms step

us to isolate a location-specific stage of numerosity processing. By contrast, decoding numerosity across hemifields allowed us to isolate a location-invariant stage of numerosity processing. In other words, by characterizing the generalization profiles and lateralization of numerosity representations at different time points, we provided direct evidence for a dual-stage mode of numerosity processing in the subitizing effect.

In line with some previous neuroimaging findings (Bankson et al., 2019; Eger et al., 2009; Eger et al., 2015; Fornaciai & Park, 2017; Hyde & Spelke, 2009; Libertus et al., 2007; Luyckx et al., 2019; Park et al., 2016; Roggeman et al., 2010; Roggeman et al., 2011; Spitzer et al., 2017; Teichmann et al., 2018), the present EEG results lent direct support to the existence of a distinction between location-specific and location-invariant numerosity coding of small object numerosities. Experiment 1 indicated that there are two subsequent stages of representation: a location-specific stage that starts at approximately 180–200 ms after stimulus and a location-invariant stage with an onset latency of 300 ms after stimulus. Crucially, the results of the additional analysis on the interaction between hemisphere and hemifield further disclosed the spatially selective organization of the first stage of numerosity coding by pointing to a predominant contralateral processing of the target numerosities in this stage. This interaction provides more selective evidence than the location-specific decoding using all channels, which might also be driven by location-invariant numerosity representations. We also observed significant decoding effects in ipsilateral hemispheres, starting around 250 ms. While decoding at later time points could also be driven by location-invariant numerosity representations, this seems unlikely for time points earlier than 300 ms, that is, before significant location-invariant decoding is observed. However, ipsilateral channels might have picked up information from the contralateral hemisphere, which could explain the decoding around 250 ms. Importantly, potential spread of information across hemispheres would increase the strength of decoding in the ipsilateral hemispheres. As a result, decoding strengths in ipsilateral and contralateral hemispheres would become more similar, which would reduce the interaction between hemisphere- and hemifield-specific decoding and thereby bias the null hypothesis. Potential spread is therefore not problematic for interpreting the significance of the interaction, which is the critical test for isolating the location-specific stage.

The nature and time course of the location-specific stage of numerosity coding resonate with previous ERP work on attention individuation of multiple targets in various contexts (e.g., enumeration, multiple object tracking, delayed match to sample tasks; Drew & Vogel, 2008; Ester et al., 2012; Foster et al., 2020; Mazza & Caramazza, 2011, 2015; Pagano et al., 2014; Vogel & Machizawa, 2004). In all these studies, a numerosity-related contralateral ERP response with a latency of approximately 200 ms (N2pc, Eimer, 2014; Luck, 2012) was found, suggesting that an attention-based mechanism of object individuation is a core component of the visual system involved in processing multiple targets (up to the three to four objects) in a variety of tasks, including enumeration. Given the presence of distracting elements in the present study, it may be that the location-specific effect measured here reflects selective tracking of relevant numerosities rather than a mechanism of numerosity perception of the total set of elements (which was kept fixed throughout the experiment). Rather than relying on a location map of the overall elements, the representation produced at this stage of analysis would reflect only the location of the crucial elements in the visual map—a representation that is crucial for subitizing in explicit enumeration tasks.

In general, the current results are in accordance with the idea that a spatially selective, attention-based mechanism may have a first important role for numerosity coding (Dehaene et al., 2003; Stoianov & Zorzi, 2012; Verguts & Fias, 2004, 2008). For instance, according to some influential proposals (e.g., Dehaene et al., 2003), the attention system could operate on numerosities as it does for other physical dimensions, such as space or time. There is evidence that numerosity can be encoded independently of and in the same fashion as other primary attributes (e.g., shape and color) (for a review, see Anobile et al., 2016; but see Dakin et al., 2011).

Despite there has not been any previous EEG attempt to directly test for the dissociation between location-specific versus location-invariant stages of small numerosity representation, the present results are in line with some previous ERP studies that separately disclosed stages with similar latencies (approximately 200 and 250 ms, respectively) as the ones seen here. The first stage has been associated with the existence of an object file system that spatially tags multiple locations at once (Hyde & Spelke, 2009), whereas the latter has been interpreted as evidence of abstract coding for number (Libertus et al., 2007). However, none of these studies have tried to investigate whether these stages were location specific. Interestingly, recent investigations (Fornaciai & Park, 2017; Park et al., 2016) have also shown an early effect (approximately 75 ms) related to the specific activation of occipital areas and interpreted this as evidence of the location-map stage where object locations are represented regardless of other physical dimensions (e.g., size). This early stage would only be activated by large numerosities (Fornaciai & Park, 2017),

whereas a later stage (approximately 180–200 ms) would instead be associated with a summation layer where the results of the location-map stage are added and an abstract representation of quantity is formed, irrespective of the numerical range used. By identifying distinct time ranges in which EEG patterns are sensitive to discriminate small numerosities in either a hemifield-specific and lateralized way or across hemifields, we could here provide direct support, in a single study, to the existence of location-sensitive versus location-invariant stages in the subitizing range.

It is unclear why the present study (as well as previous ones, e.g., Hyde & Spelke, 2009) did not reliably find a location-specific effect already in the early time windows (<80 ms, as in Fornaciai & Park, 2017; Park et al., 2016; although we observed significant location-specific decoding shortly after 100 ms and a trend for a significant interaction around the same time). Although future research will address this aspect in more detail, we suggest that the early effect reflects the operation of a stage that relies on a location map of the entire set of objects presented and of their variation in numerosity (as in the Fornaciai & Park, 2017; Park et al., 2016), which was not the case for the present study where the overall number of elements did not vary across trials. This would further reinforce the idea that the location-specific effect measured found here reflects attention selection of relevant numerosities rather than an early mechanism of numerosity perception of the total set of elements.

Finally, we found that the early location-specific and later location-invariant stage were associated with different topographical distributions, peaking around posterior occipital channels and more anterior parietal channels, respectively. This might suggest that the two stages are processed by different neural substrates. Although the EEG topography of the numerosity decoding effects does not allow for a precise anatomical localization, it appears plausible (based on related fMRI findings) that location-specific effects originate from occipitotemporal or occipitoparietal areas and location-invariant effects originate from more anterior, parietal areas (Eger et al., 2009; Roggeman et al., 2011; Wurm et al., 2019).

Overall, Experiment 1 provided compelling evidence that small numerosities are processed via an attention-based stage that initially takes into account the location of the to-be-enumerated elements, followed by a stage that is invariant to the elements' location and (likely) represents numerosities in a more abstract way. The location-specific stage (as identified by the more conservative interaction, 224–380) remains activated overlapping with the location-invariant stage (starting around 300 ms) for at least 60 ms.

Experiment 2 further specified the nature of the numerosity coding stages involved in the task used in the present study. The results showed that there was no numerosity-related modulation when numerosity was irrelevant for the task. Importantly, we can rule out that this null effect could be due to a lack of power: Bayesian comparisons revealed that many points during the location-specific and location-invariant stages identified in Experiment 1 do not show evidence for trends or even stronger evidence for the null hypothesis that effects are not different than chance. Moreover, location-specific and location-invariant stages in Experiment 1 could still be identified after reducing the sample size to $N = 12$ (as in Experiment 2) using a bootstrapping approach. Most importantly, we observed highly significant decoding in Experiment 2 when target numerosities (one, two, or three targets) were discriminated from zero-target trials, that is, when the classifier could rely on the task-relevant dimension. This finding perfectly matches the typical context in which subitizing emerges, namely, enumeration tasks where the observers have to explicitly report the numerosity of the relevant elements (e.g., Trick & Pylyshyn, 1993). Therefore, the findings suggest that the location-specific and location-invariant components seen in Experiment 1 were not merely triggered by an automatic, passive recording of numerosities and their variation (as well as other, continuous magnitudes related to this variation). Likewise, these results further rule out alternative explanations for the numerosity effect observed in Experiment 1, such as those related to passive recording of changes in continuous dimensions (e.g., density and local area) that typically correlate with variations in numerosity. The existence of a mechanism for coding numerosity independently of other continuous magnitudes (e.g., size and area) is still debated (for a recent review, see Leibovich et al., 2017). However, the results of Experiment 2 indicated that (passive) recording of continuous magnitudes is insufficient to explain the effects found in Experiment 1. Altogether, the results of Experiments 1 and 2 point out that the decoding of numerosity addressed in the present study only pertains to contexts where numerosity is task relevant, rather than to passive viewing of numerosities.

5 | CONCLUSION

Using EEG-based MVPA, we disentangled location-specific and location-invariant stages of small numerosity representation in (explicit) enumeration. The results suggest that numerosity coding in subitizing is strongly grounded on an attention-based stage that operates

according to coordinates of a location map. This stage remains active overlapping with the subsequent activation of a location-invariant stage, where a complete abstract representation of numerosity is finalized by the brain. The approach taken in the present study could successfully be extended to larger numerosities and for different task requirements in order to fully disclose the neural architecture of number coding.

ACKNOWLEDGEMENTS

We would like to thank Manuela Piazza for valuable feedback on the manuscript and Davide Tabarelli for methodological feedback. This research was supported by the Provincia Autonoma di Trento and the Fondazione Cassa di Risparmio di Trento e Rovereto.

CONFLICT OF INTEREST

The authors declare no competing interests.

AUTHOR CONTRIBUTIONS

M.F.W., C.F.T., and V.M. planned the analyses and wrote the manuscript, and M.F.W. and C.F.T. analyzed the data.

PEER REVIEW

The peer review history for this article is available at https://publons.com/publon/10.1111/ejn.15352.

DATA AVAILABILITY STATEMENT

Preprocessed EEG data are deposited at OSF (https://osf.io/kb23q/). Analysis code is available upon reasonable request.

ORCID

Moritz F. Wurm https://orcid.org/0000-0003-4358-9815
Chiara F. Tagliabue https://orcid.org/0000-0002-4152-1668

REFERENCES

Anobile, G., Cicchini, G. M., & Burr, D. C. (2016). Number as a primary perceptual attribute: A review. *Perception*, *45*, 5–31. https://doi.org/10.1177/0301006615602599

Ansari, D., Lyons, I. M., van Eimeren, L., & Xu, F. (2007). Linking visual attention and number processing in the brain: The role of the temporo-parietal junction in small and large symbolic and nonsymbolic number comparison. *Journal of Cognitive Neuroscience*, *19*, 1845–1853. https://doi.org/10.1162/jocn.2007.19.11.1845

Bankson, B. B., Janini, D., & Baker, C. I. (2019). Whole-brain MEG decoding of symbolic and non-symbolic number stimuli reveals primarily format-dependent representations. bioRxiv, 731687.

Burr, D., & Ross, J. (2008). A visual sense of number. *Current Biology*, *18*, 425–428. https://doi.org/10.1016/j.cub.2008.02.052

Cavanagh, P., & Alvarez, G. A. (2005). Tracking multiple targets with multifocal attention. *Trends in Cognitive Sciences*, *9*, 349–354. https://doi.org/10.1016/j.tics.2005.05.009

Dakin, S. C., Tibber, M. S., Greenwood, J. A., & Morgan, M. J. (2011). A common visual metric for approximate number and density. *Proceedings of the National Academy of Sciences*, *108*, 19552–19557. https://doi.org/10.1073/pnas.1113195108

Dehaene, S., & Changeux, J. P. (1993). Development of elementary numerical abilities: A neuronal model. *Journal of Cognitive Neuroscience*, *5*, 390–407. https://doi.org/10.1162/jocn.1993.5.4.390

Dehaene, S., Piazza, M., Pinel, P., & Cohen, L. (2003). Three parietal circuits for number processing. *Cognitive Neuropsychology*, *20*, 487–506. https://doi.org/10.1080/02643290244000239

Delorme, A., & Makeig, S. (2004). EEGLAB: An open source toolbox for analysis of single-trial EEG dynamics including independent component analysis. *Journal of Neuroscience Methods*, *134*, 9–21. https://doi.org/10.1016/j.jneumeth.2003.10.009

Drew, T., & Vogel, E. K. (2008). Neural measures of individual differences in selecting and tracking multiple moving objects. *The Journal of Neuroscience*, *28*, 4183–4191. https://doi.org/10.1523/JNEUROSCI.0556-08.2008

Eger, E., Michel, V., Thirion, B., Amadon, A., Dehaene, S., & Kleinschmidt, A. (2009). Deciphering cortical number coding from human brain activity patterns. *Current Biology*, *19*, 1608–1615. https://doi.org/10.1016/j.cub.2009.08.047

Eger, E., Pinel, P., Dehaene, S., & Kleinschmidt, A. (2015). Spatially invariant coding of numerical information in functionally defined subregions of human parietal cortex. *Cerebral Cortex*, *25*, 1319–1329. https://doi.org/10.1093/cercor/bht323

Eimer, M. (1996). The N2pc component as an indicator of attentional selectivity. *Electroencephalography and Clinical Neurophysiology*, *99*, 225–234. https://doi.org/10.1016/0013-4694(96)95711-9

Eimer, M. (2014). The neural basis of attentional control in visual search. *Trends in Cognitive Sciences*, *18*, 526–535. https://doi.org/10.1016/j.tics.2014.05.005

Ester, E. F., Drew, T., Klee, D., Vogel, E. K., & Awh, E. (2012). Neural measures reveal a fixed item limit in subitizing. *The Journal of Neuroscience*, *32*, 7169–7177. https://doi.org/10.1523/JNEUROSCI.1218-12.2012

Feigenson, L., Dehaene, S., & Spelke, E. (2004). Core systems of number. *Trends in Cognitive Sciences*, *8*, 307–314. https://doi.org/10.1016/j.tics.2004.05.002

Fornaciai, M., Brannon, E. M., Woldorff, M. G., & Park, J. (2017). Numerosity processing in early visual cortex. *NeuroImage*, *157*, 429–438. https://doi.org/10.1016/j.neuroimage.2017.05.069

Fornaciai, M., & Park, J. (2017). Distinct neural signatures for very small and very large numerosities. *Frontiers in Human Neuroscience*, *11*, 21.

Foster, J. J., Bsales, E. M., & Awh, E. (2020). Covert spatial attention speeds target individuation. *Journal of Neuroscience*, *40*, 2717–2726. https://doi.org/10.1523/JNEUROSCI.2962-19.2020

Harvey, B. M., & Dumoulin, S. O. (2017). Can responses to basic non-numerical visual features explain neural numerosity responses? *NeuroImage*, *149*, 200–209. https://doi.org/10.1016/j.neuroimage.2017.02.012

Harvey, B. M., Fracasso, A., Petridou, N., & Dumoulin, S. O. (2015). Topographic representations of object size and relationships

with numerosity reveal generalized quantity processing in human parietal cortex. *Proceedings of the National Academy of Sciences of the United States of America*, *112*, 13525–13530. https://doi.org/10.1073/pnas.1515414112

Hyde, D. C., & Spelke, E. S. (2009). All numbers are not equal: An electrophysiological investigation of small and large number representations. *Journal of Cognitive Neuroscience*, *21*, 1039–1053. https://doi.org/10.1162/jocn.2009.21090

Kaufman, E. L., Lord, M. W., Reese, T. W., & Volkmann, J. (1949). The discrimination of visual number. *The American Journal of Psychology*, *62*, 498–525. https://doi.org/10.2307/1418556

Leibovich, T., Katzin, N., Harel, M., & Henik, A. (2017). From "sense of number" to "sense of magnitude": The role of continuous magnitudes in numerical cognition. *Behavioral and Brain Sciences*, *40*, e164. https://doi.org/10.1017/S0140525X16000960

Libertus, M. E., Woldorff, M. G., & Brannon, E. M. (2007). Electrophysiological evidence for notation independence in numerical processing. *Behavioral and Brain Functions*, *3*, 1. https://doi.org/10.1186/1744-9081-3-1

Lopez-Calderon, J., & Luck, S. J. (2014). ERPLAB: An open-source toolbox for the analysis of event-related potentials. *Frontiers in Human Neuroscience*, *8*, 213.

Luck, S. J. (2012). Electrophysiological correlates of the focusing of attention within complex visual scenes: N2pc and related ERP components.

Luyckx, F., Nili, H., Spitzer, B., & Summerfield, C. (2019). Neural structure mapping in human probabilistic reward learning. *eLife*, *8*, e42816. https://doi.org/10.7554/eLife.42816

Mandler, G., & Shebo, B. J. (1982). Subitizing: An analysis of its component processes. *Journal of Experimental Psychology: General*, *111*, 1.

Mazza, V., & Caramazza, A. (2011). Temporal brain dynamics of multiple object processing: The flexibility of individuation. *PLoS ONE*, *6*, e17453. https://doi.org/10.1371/journal.pone.0017453

Mazza, V., & Caramazza, A. (2015). Multiple object individuation and subitizing in enumeration: A view from electrophysiology. *Frontiers in Human Neuroscience*, *9*, 162.

Mazza, V., Pagano, S., & Caramazza, A. (2013). Multiple object individuation and exact enumeration. *Journal of Cognitive Neuroscience*, *25*, 697–705. https://doi.org/10.1162/jocn_a_00349

Meck, W. H., & Church, R. M. (1983). A mode control model of counting and timing processes. *Journal of Experimental Psychology: Animal Behavior Processes*, *9*, 320.

Oostenveld, R., Fries, P., Maris, E., & Schoffelen, J.-M. (2011). FieldTrip: Open source software for advanced analysis of MEG, EEG, and invasive electrophysiological data. *Computational Intelligence and Neuroscience*, *2011*, 156869.

Oosterhof, N. N., Connolly, A. C., & Haxby, J. V. (2016). CoSMoMVPA: Multi-modal multivariate pattern analysis of neuroimaging data in Matlab/GNU octave. *Frontiers in Neuroinformatics*, *10*, 27.

Pagano, S., Lombardi, L., & Mazza, V. (2014). Brain dynamics of attention and working memory engagement in subitizing. *Brain Research*, *1543*, 244–252. https://doi.org/10.1016/j.brainres.2013.11.025

Park, J., DeWind, N. K., Woldorff, M. G., & Brannon, E. M. (2016). Rapid and direct encoding of numerosity in the visual stream. *Cerebral Cortex*, *26*, 748–763. https://doi.org/10.1093/cercor/bhv017

Piazza, M. (2010). Neurocognitive start-up tools for symbolic number representations. *Trends in Cognitive Sciences*, *14*, 542–551. https://doi.org/10.1016/j.tics.2010.09.008

Piazza, M., Izard, V., Pinel, P., Le Bihan, D., & Dehaene, S. (2004). Tuning curves for approximate numerosity in the human intraparietal sulcus. *Neuron*, *44*, 547–555. https://doi.org/10.1016/j.neuron.2004.10.014

Pylyshyn, Z. W. (2001). Visual indexes, preconceptual objects, and situated vision. *Cognition*, *80*, 127–158. https://doi.org/10.1016/S0010-0277(00)00156-6

Roggeman, C., Fias, W., & Verguts, T. (2010). Salience maps in parietal cortex: Imaging and computational modeling. *NeuroImage*, *52*, 1005–1014. https://doi.org/10.1016/j.neuroimage.2010.01.060

Roggeman, C., Santens, S., Fias, W., & Verguts, T. (2011). Stages of nonsymbolic number processing in occipitoparietal cortex disentangled by fMRI adaptation. *The Journal of Neuroscience*, *31*, 7168–7173. https://doi.org/10.1523/JNEUROSCI.4503-10.2011

Spitzer, B., Waschke, L., & Summerfield, C. (2017). Selective overweighting of larger magnitudes during noisy numerical comparison. *Nature Human Behaviour*, *1*, 145. https://doi.org/10.1038/s41562-017-0145

Stoianov, I., & Zorzi, M. (2012). Emergence of a 'visual number sense' in hierarchical generative models. *Nature Neuroscience*, *15*, 194–196. https://doi.org/10.1038/nn.2996

Teichmann, L., Grootswagers, T., Carlson, T., & Rich, A. N. (2018). Decoding digits and dice with magnetoencephalography: Evidence for a shared representation of magnitude. *Journal of Cognitive Neuroscience*, *30*, 999–1010. https://doi.org/10.1162/jocn_a_01257

Trick, L. M., & Pylyshyn, Z. W. (1993). What enumeration studies can show us about spatial attention: Evidence for limited capacity preattentive processing. *Journal of Experimental Psychology. Human Perception and Performance*, *19*, 331–351. https://doi.org/10.1037/0096-1523.19.2.331

Trick, L. M., & Pylyshyn, Z. W. (1994). Why are small and large numbers enumerated differently—A limited-capacity preattentive stage in vision. *Psychological Review*, *101*, 80–102. https://doi.org/10.1037/0033-295X.101.1.80

Verguts, T., & Fias, W. (2004). Representation of number in animals and humans: A neural model. *Journal of Cognitive Neuroscience*, *16*, 1493–1504. https://doi.org/10.1162/0898929042568497

Verguts, T., & Fias, W. (2008). Symbolic and nonsymbolic pathways of number processing. *Philosophical Psychology*, *21*, 539–554. https://doi.org/10.1080/09515080802285545

Vetter, P., Butterworth, B., & Bahrami, B. (2011). A candidate for the attentional bottleneck: Set-size specific modulation of the right TPJ during attentive enumeration. *Journal of Cognitive Neuroscience*, *23*, 728–736. https://doi.org/10.1162/jocn.2010.21472

Viswanathan, P., & Nieder, A. (2020). Spatial neuronal integration supports a global representation of visual numerosity in primate association cortices. *Journal of Cognitive Neuroscience*, *32*, 1184–1197. https://doi.org/10.1162/jocn_a_01548

Vogel, E. K., & Machizawa, M. G. (2004). Neural activity predicts individual differences in visual working memory capacity. *Nature*, *428*, 748–751. https://doi.org/10.1038/nature02447

Wurm, M. F., Porter, K. B., & Caramazza, A. (2019). Individuation of parts of a single object and multiple distinct objects relies on a common neural mechanism in inferior intraparietal sulcus. *Cortex*, *121*, 1–15. https://doi.org/10.1016/j.cortex.2019.08.012

Xu, Y., & Chun, M. M. (2009). Selecting and perceiving multiple visual objects. *Trends in Cognitive Sciences*, *13*, 167–174. https://doi.org/10.1016/j.tics.2009.01.008

Zorzi, M., Stoianov, I., & Umiltà, C. (2005). Computational modeling of numerical cognition. In *Handbook of mathematical cognition* (Vol. 19, pp. 67–84). London: Psychology Press.

SUPPORTING INFORMATION

Additional supporting information may be found online in the Supporting Information section at the end of this article.

How to cite this article: Wurm, M. F., Tagliabue, C. F., & Mazza, V. (2021). Decoding location-specific and location-invariant stages of numerosity processing in subitizing. *European Journal of Neuroscience*, *54*(3), 4971–4984. https://doi.org/10.1111/ejn.15352